

## Electronic band structure of epitaxial $\sqrt{3} \times \sqrt{3}R30^\circ \epsilon\text{-FeSi}(111)/\text{Si}(111)$

J. J. Hinarejos, P. Segovia, J. Alvarez, G. R. Castro, E. G. Michel, and R. Miranda

*Departamento de Física de la Materia Condensada and Instituto Universitario de Ciencia de Materiales "Nicolás Cabrera,"  
Universidad Autónoma de Madrid, 28049 Madrid, Spain*

(Received 22 May 1997)

The electronic band structure of  $\sqrt{3} \times \sqrt{3}R30^\circ \epsilon\text{-FeSi}(111)$  epitaxially grown on Si(111) has been probed by angle-resolved polarization-sensitive ultraviolet photoemission in the energy range  $8 \text{ eV} \leq h\nu \leq 30 \text{ eV}$ . The bands were mapped along the  $\Gamma\text{-R}$  direction of the Brillouin zone for different detection geometries. A comparison with theoretical calculations reveals a good agreement of the overall features at room temperature. A sharp peak close to the Fermi energy was observed. Its origin is discussed taking into account both conventional and Kondo-insulator models currently considered to explain the properties of  $\epsilon\text{-FeSi}$ . [S0163-1829(98)09303-5]

The epitaxial growth of iron silicides on silicon has been a matter of interest during the last years. Several authors have investigated the growth of epitaxial phases,<sup>1-5</sup> corresponding to distinct Fe:Si stoichiometries and crystalline structures.  $\epsilon\text{-FeSi}$ , which is the bulk stable phase corresponding to a 1:1 Fe:Si stoichiometry, crystallizes in a simple cubic lattice that is the prototype  $B20$  structure (space group  $T^4\text{-}P2_13$ ).<sup>6</sup> It contains four FeSi molecules in the unit cell (see Fig. 1), and due to the low symmetry of the  $P2_13$  group, it is especially difficult to visualize. Mattheiss and Hamann<sup>7</sup> have proposed that for the purposes of visualization, the  $B20$  structure could be imagined as a strong distortion of a hypothetical FeSi rocksalt structure (see Ref. 7 for details). The only symmetry operation of the  $P2_13$  group (in addition to the cubic ternary axes), are screw axes along the cubic directions. Fe and Si atoms are located in equivalent positions  $(x, x, x)$ ,  $(\frac{1}{2} + x, \frac{1}{2} - x, \bar{x})$ ,  $(\bar{x}, \frac{1}{2} + x, \frac{1}{2} - x)$ , and  $(\frac{1}{2} - x, \bar{x}, \frac{1}{2} + x)$ , with  $x_{\text{Fe}} = 0.137 \pm 0.002$  and  $x_{\text{Si}} = 0.842 \pm 0.005$  (in units of the lattice spacing  $a = 4.488\text{-}4.483 \text{ \AA}$ ).<sup>6</sup> Thus, along the (111) direction planes containing only Fe or only Si atoms are alternated (see Fig. 1).

In addition to  $\epsilon\text{-FeSi}$ , the growth of metastable phases with 1:1 stoichiometry has been also reported.<sup>4,8</sup> Such phases do not exist in nature, but can be stabilized during the epitaxy due to a better lattice matching with Si than the corresponding bulk phase (for the same Fe:Si stoichiometry). By this method, a FeSi(CsCl) phase was grown.<sup>4</sup> On the other hand, thin films ( $< 50 \text{ \AA}$  thickness) of  $\epsilon\text{-FeSi}$  were grown on Si(100) (Refs. 2,9) and Si(111) (Refs. 3,5,8,10-12) by several groups, but their electronic structure was not characterized in detail, mainly because previous works concentrated in metastable phases. When iron silicides are grown on Si(111),  $\epsilon\text{-FeSi}$  can be obtained in the form of a fairly well ordered, (111)-oriented film, or in the form of a polycrystalline film, the latter being the only form for very thick films ( $> 50 \text{ \AA}$ ). For thickness below  $25 \text{ \AA}$ ,  $\epsilon\text{-FeSi}$  has been associated with a  $\sqrt{3} \times \sqrt{3}R30^\circ$  reconstruction,<sup>5,10-12</sup> although most of the evidence for this assignment was indirect. If one recalls the  $\epsilon\text{-FeSi}$  structure, the interatomic distances within (111) planes along  $[0\bar{1}1]$  direction are approximately  $\sqrt{3}$  times the Si-Si distances at the (111) surface along  $[11\bar{2}]$

direction ( $6.35 \text{ \AA}$  vs  $6.65 \text{ \AA}$ ), i.e., the growth of epitaxial  $\epsilon\text{-FeSi}(111)$  would give rise to a  $\sqrt{3} \times \sqrt{3}R30^\circ$  structure when referred to the  $1 \times 1$  Si(111) surface lattice. The epitaxial relationships found for these films are  $\epsilon\text{-FeSi}(111) \parallel \text{Si}(111)$  and  $\epsilon\text{-FeSi}(0\bar{1}0) \parallel \text{Si}(11\bar{2})$ .<sup>1,13</sup>

The interest of bulk and epitaxial  $\epsilon\text{-FeSi}$  has increased since it was proposed by Mason *et al.*<sup>14</sup> that it might represent the first example of a Kondo insulator based on  $d$ -type electrons (namely, the  $3d$  Fe band). It might be useful to recall some of the properties of  $\epsilon\text{-FeSi}$ . The first studies on this compound date back to the late 1930's, when it was discovered that its magnetic susceptibility increased with temperature above room temperature, passing through a broad maximum at  $\sim 500 \text{ K}$ .<sup>15</sup> Although the easiest explanation could be an antiferromagnetic transition, neutron diffraction, Mössbauer effect, and Knight shift measurements failed to find any sort of ordered moments. Thus, FeSi pre-

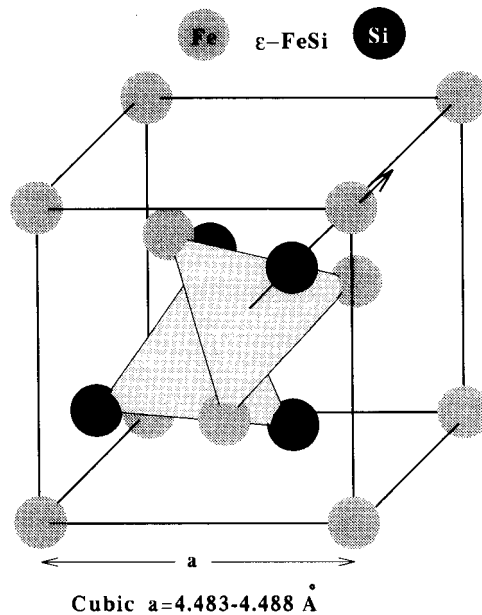


FIG. 1. Crystalline structure of  $\epsilon\text{-FeSi}$ . Two (111) planes are shaded, and the  $[111]$  direction is marked with an arrow.

sents a unique magnetic behavior, when compared, for instance, with  $\text{MnSi}$ <sup>16</sup> or  $\text{CoSi}$ ,<sup>17</sup> without being magnetically ordered. Several models have been put forward to explain the dependence of the susceptibility. Jaccarino *et al.*<sup>15</sup> proposed two different (but in fact very similar) models, based on the existence of two states symmetrically placed around the chemical potential. We refer the reader to Ref. 15 for more details. An alternative explanation was proposed later by Takahashi and Moriya,<sup>18</sup> who introduced strong local Coulomb interaction, which was shown to promote enhanced thermally-induced spin fluctuations for a two narrow band ( $\sim 1$  eV) model, keeping a gap. This image was supported by inelastic neutron scattering measurements.<sup>19</sup> As we mentioned above, Mason *et al.* have pointed out in a recent study<sup>14</sup> that the peculiar magnetic behavior of  $\text{FeSi}$  was similar to the spin-fluctuation spectrum of the Kondo insulator  $\text{Ce}_x\text{Ni}_{1-x}\text{Sn}$ . These authors suggested that  $3d$  electrons of  $\epsilon\text{-FeSi}$  could behave in a similar way as  $4f$  electrons do in conventional rare-earth-based Kondo insulators. In this model, the  $3d$  electrons should hybridize with an extended, itinerant conduction band formed by  $\text{Si } 3sp^3$  electrons. This would be an unexpected behavior, since the  $3d$  wave functions are usually rather broad (compared to  $4f$ ).<sup>23</sup> In spite of such objections, recent experimental data<sup>20–22</sup> are described well by a two-band model compatible with a Kondo insulator. From the point of view of the band structure, linear-augmented plane-wave (LAPW) calculations carried out in the local-density approximation (LDA) by Mattheiss and Hamann<sup>7</sup> have predicted a gap of  $\sim 0.11$  eV and a bandwidth roughly a factor 10 too wide (0.5 vs 0.06 eV) to explain the thermodynamics and resistivity properties.<sup>20</sup> Nevertheless, and in spite of the differences between the Kondo-insulator model and the enhanced spin-fluctuation model, theoretical band results appear to be consistent with both. Recent augmented spherical wave (ASW) calculations carried out in the LDA scheme have also obtained a  $\sim 0.1$  eV band gap.<sup>23</sup>

We set out to characterize the electronic band structure of epitaxial  $\epsilon\text{-FeSi}(111)$  by polarization-sensitive, energy-dependent, angle-resolved ultraviolet photoemission (ARUPS), with the aim of establishing a comparison with theoretical calculations and determining the relevant experimental features of the band structure of  $\epsilon\text{-FeSi}(111)$  along the  $\Gamma R$  direction. This is the highest symmetry direction for  $P2_13$ , but due to the stacking sequence along it, it is difficult to prepare a single-crystalline surface of this orientation. On the other hand, the reduced dimensionality of a thin film enhances correlation effects. These two arguments lead us to investigate epitaxial  $\epsilon\text{-FeSi}$ . The electronic structure of bulk, single-crystalline  $\epsilon\text{-FeSi}(100)$  is discussed elsewhere.<sup>25</sup> Previous photoemission results have concentrated in different properties, and not in the band topology itself, either due to lack of angular or energy resolution, or because the samples were polycrystalline or without a well-defined crystal plane.<sup>24,26–28,22</sup> The adequacy of existing models to explain ARUPS results can shed light on the fundamental properties of  $\epsilon\text{-FeSi}$ .

The experiments have been carried out in an ultrahigh-vacuum chamber permanently located at the exit of a SEYA-1m monochromator receiving synchrotron light from the DORIS III storage ring of the Hamburger Synchrotronstrahlungslabor (HASYLAB) at Deutsches Elektronen-

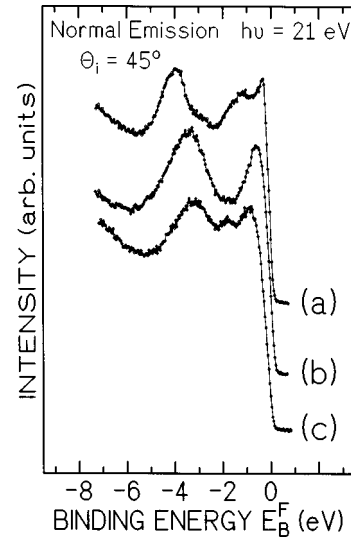


FIG. 2. Normal emission ARUPS spectra ( $h\nu=21$  eV) for: (a),  $\sqrt{3}\times\sqrt{3}R30^\circ\text{-}\epsilon\text{-FeSi}(111)$ ; (b)  $1\times 1\text{-FeSi}(\text{CsCl})$ ; (c)  $2\times 2\text{-FeSi}(\text{CsCl})$ .

synchrotron (DESY). It was equipped with facilities for low-energy electron diffraction (LEED), auger electron spectroscopy (AES), and ARUPS. The ARUPS spectra were recorded with a hemispherical analyzer mounted on an ultrahigh-vacuum goniometer, operated at an energy resolution going from 0.1 eV at  $h\nu=8$  eV to 0.23 eV at  $h\nu=27$  eV. The angular resolution was  $\pm 2^\circ$ , and the base pressure of the system was  $5\times 10^{-11}$  Torr. All surfaces prepared as described above consistently displayed an intense emission from  $\text{Si}(111)$  surface states and a sharp  $7\times 7$  LEED pattern.  $n\text{-Si}(111)$ , mirror-polished single-crystalline samples (resistivity 0.03–0.05  $\Omega$  cm) were cleaned by annealing at  $1100^\circ\text{C}$  after long time degassing at lower temperatures. Silicide films were prepared by solid phase epitaxy (SPE). To this end, Fe was deposited in the preparation chamber from an Fe wire resistively heated. The coverage was measured with a quartz microbalance, and cross checked determining the AES intensity ratios of Si and Fe peaks at 92 and 56 eV, respectively. All cited coverages are subject to an estimated error of  $\pm 20\%$ . Samples identically prepared in a different experimental chamber consistently showed an Fe:Si stoichiometry of 1:1, as determined by quantitative x-ray photoemission spectroscopy.<sup>2,3</sup>

In addition to  $\epsilon\text{-FeSi}$ , the bulk stable phase corresponding to a 1:1 Fe:Si stoichiometry, the growth of metastable  $\text{FeSi}(\text{CsCl})$  is possible on  $\text{Si}(111)$ .<sup>4</sup> This phase can be obtained with different surface terminations:  $1\times 1$  (corresponding to approximately an abrupt truncation of the  $\text{FeSi}(\text{CsCl})$  crystal),<sup>29</sup> and  $2\times 2$  (associated to a Si-atom surface arrangement). Figure 2 presents ARUPS spectra characteristic of the three phases ( $h\nu=21$  eV,  $45^\circ$  incidence angle on light, normal emission). The details of the features observed in  $\text{FeSi}(\text{CsCl})$  spectra is discussed in detail elsewhere.<sup>29</sup> A minor contribution from this phase cannot be excluded on the basis of our data alone, but we note here that, at variance with the other silicides of close stoichiometry, the  $\sqrt{3}\times\sqrt{3}R30^\circ$  structure presents a characteristic narrow peak close to  $E_F$ . The appearance of this peak denotes a significant density of states (DOS) in a narrow energy range at the

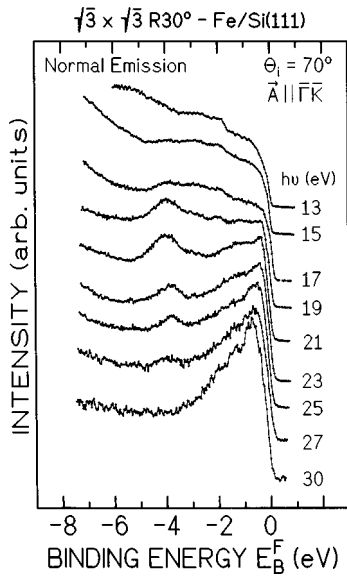


FIG. 3. Normal emission ARUPS spectra for a range of different photon energies ( $8 \leq h\nu \leq 27$  eV), for  $p$  polarization geometry.

gap edge. The existence of a similar peak was reported previously by Park *et al.*<sup>22</sup> We will come back to it later. On the basis of the characteristic features of the spectra (see Fig. 2) it is thus possible to unambiguously identify the  $\sqrt{3} \times \sqrt{3} R30^\circ$  structure.

Figure 3 presents a series of spectra obtained for different photon energies at normal emission and under  $p$  polarization conditions. Similar series were measured for  $s$  polarization conditions (not shown). The kinetic energies corresponding to well-defined peaks have been converted into  $k_\perp$  values assuming a parabolic free-electron-like final-state band, and an inner potential of  $V_0 = 13.0$  eV (measured from  $E_F$ ). This value has been obtained from the muffin-tin zero of LDA-LAPW band-structure calculations.<sup>7</sup> As is usual, a change of

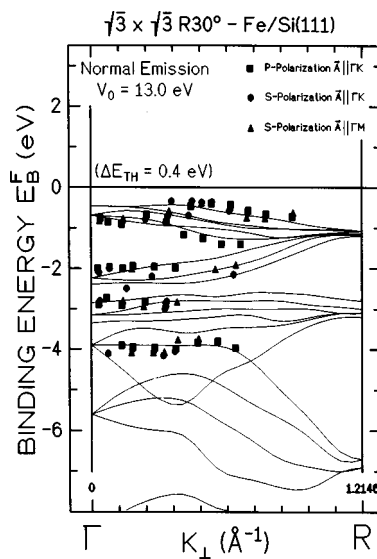


FIG. 4. Measured binding energies vs  $k_\perp$  for  $\sqrt{3} \times \sqrt{3} R30^\circ$ - $\epsilon$ -FeSi(111), calculated using a direct transition model with a free-electron final-state band. An inner potential of 13.0 eV was used. The data have been reduced to the first Brillouin zone. Continuous lines are a theoretical calculation from Ref. 7.

the value assumed for  $V_0$  within reasonable ranges would only slightly alter the band topology described by the experimental points presented in Fig. 4, reduced to the first Brillouin zone. We may note that due to the low symmetry of the space group of  $\epsilon$ -FeSi, which contains no mirror planes, usual selection rules in cubic crystals based on  $s$ - and  $p$ -polarization geometries, are not effective here for electronic bulk states. This fact is reflected in the experimental data, where no significant difference between the  $s$  and  $p$  sets of points is observed. As we did not detect any feature that may correspond to surface states or surface resonances, all peaks were assigned to bulk states. Figure 4 presents also the theoretical LDA-LAPW bands from Ref. 7, shifted by 0.4 eV to higher binding energy (BE) in order to better reproduce the experimental points. A rigid shift of this amount is within reasonable limits, due to the difficulty of most calculations to account for exchange-correlation effects.

The theoretical bands in Fig. 4 appear grouped together in several bunches where the energy difference between the bands is very small [e.g., at  $\Gamma$  we find bunches at  $\sim 0.8$  eV, 2.2 eV, 3 eV, and 4 eV BE]. This behavior is typical of low-symmetry crystals, and is due to the band split off associated to degeneracy lifting.<sup>7</sup> Due to the limited experimental resolution, only one or at most two resolved peaks can be observed for each bunch of bands. Taking into account this limitation, the theoretical bands describe well all the experimental points. In particular, the value of 1.2 eV between the first two bunches at  $\Gamma$ , and the convergence of these two groups at  $\sim 0.5 \Gamma R$  are well reproduced by the theory. This agreement allows a definite identification of the  $\sqrt{3} \times \sqrt{3} R30^\circ$  structure with  $\epsilon$ -FeSi from the electronic point of view. We note that the area close to  $R$  point was not probed due to limitations of the photon energy range available. We have also compared our results with self-consistent augmented spherical wave (ASW) calculations incorporating exchange and correlation effects in the LDA.<sup>23</sup> The agreement is also good, which could be foreseen taking into account the similarity between the LDA-ASW bands<sup>23</sup> and LDA-LAPW bands.<sup>7</sup>

Several experimental results from different techniques can be well understood assuming the existence of extremely narrow valence and conduction bands,<sup>15,20</sup> whose widths should be small compared with the gap. The extreme narrowness of these bands [ $\sim 60$  meV (Ref. 20)] is below the experimental resolution in conventional ARUPS experiments, and their existence cannot be excluded on the basis of our results, which exhibit bandwidths of  $\sim 0.5$  eV, in good agreement with LDA-LAPW calculations.<sup>7</sup> Another drawback to perform this characterizations at room temperature (RT) comes from the small width of the band gap, which would give rise to a smoothed structure around  $E_F$  at 300 K.<sup>24</sup>

One of the most conspicuous features of the spectra, not present in any other iron silicide,<sup>29</sup> is a narrow, intense peak localized at  $\sim 0.25$  eV BE, with a full-width at half-maximum close to our resolution limit ( $\sim 0.1$  eV). In fact, the calculated band structure of  $\epsilon$ -FeSi predicts a large density of rather flat bands close to  $E_F$ , but a comparison with the calculated DOS (Refs. 7,23) reveals an increased DOS close to  $E_F$  with respect to calculations. In any case, the nature and origin of these states deserves some more analysis. The peak appears at  $\sim 0.6 \Gamma R$ , i.e., somewhat behind the

band maximum predicted by calculations [ $\sim 0.3 \Gamma R$  (Refs. 7,23)]. This type of peaks are considered a strong evidence for a Kondo insulator description. Previous low-temperature photoemission experiments on samples without well-defined crystalline orientation<sup>22</sup> have shown the presence of a similar peak with a spectacular intensity enhancement upon temperature decreasing down to 25 K. This is an important finding that supports again the ascription of this compound into the class of highly correlated electron materials. Due to the extremely small band-gap value determined by photoemission (5 meV), a quasimetallic behavior was found at room temperature.<sup>24</sup> Interestingly, the peak at  $\sim 0.25$  eV in our experiments is not a proper DOS feature, since it appears well localized in the Brillouin zone along  $\Gamma R$ , and quickly disappears for off-normal emission. Although in a simple model one would expect a purely collective character, one should take into account the more delocalized nature of Fe 3d electrons compared to 4f electrons, and also that even for the latter bandlike character has been reported in some cases.<sup>30</sup> A definite assignment will certainly require further experimental characterization. The observation of the peak at

RT was much more difficult in previous experiments using bulk samples.<sup>22</sup> This enhancement can be explained either by the quasi-two-dimensional nature of the thin  $\epsilon$ -FeSi epitaxial film, or by our probing of a single crystalline, (111)-oriented sample.

In conclusion, the experimental band structure of the  $\sqrt{3} \times \sqrt{3} R30^\circ$  iron silicide phase has been determined for epitaxial films grown on Si(111). The results present a good agreement with theoretical calculations for  $\epsilon$ -FeSi(111), and allow a definite identification with this compound on the basis of the electronic structure. A sharp peak close to the Fermi energy has been detected, which is compatible with the behavior expected for a Kondo insulator.

This work was supported by DGICYT through Grant Nos. PB91-0929 and PB94-1527, and by the Large Scale Installations Program of the European Union. J.J.H. thanks the Spanish Ministry of Education and Science for financial support.

<sup>1</sup>J. Chevrier *et al.*, Appl. Surf. Sci. **56-58**, 438 (1992).

<sup>2</sup>J. Alvarez *et al.*, Phys. Rev. B **45**, 14 042 (1992).

<sup>3</sup>J. Alvarez *et al.*, Surf. Sci. **287/288**, 490 (1993).

<sup>4</sup>H. von Känel *et al.*, Phys. Rev. B **45**, 13 807 (1992).

<sup>5</sup>H. von Känel *et al.*, Appl. Surf. Sci. **70/71**, 559 (1993).

<sup>6</sup>L. Pauling and M. Soldate, Acta Crystallogr. **1**, 212 (1948).

<sup>7</sup>L.F. Mattheiss and D.R. Hamann, Phys. Rev. B **47**, 13 114 (1993).

<sup>8</sup>J. Alvarez *et al.*, J. Vac. Sci. Technol. **11**, 929 (1993).

<sup>9</sup>W. Raunau, H. Niehus, and G. Comsa, Surf. Sci. **284**, L375 (1993).

<sup>10</sup>Y.L. Gavriljuk, L.Y. Kachonova, and V.G. Lifshits, Surf. Sci. Lett. **256**, L589 (1991).

<sup>11</sup>X. Wallart, J.P. Nys, and C. Tételin, Phys. Rev. B **49**, 5714 (1994).

<sup>12</sup>W. Raunau *et al.*, Surf. Sci. **286**, 203 (1993).

<sup>13</sup>N. Onda *et al.*, J. Cryst. Growth **127**, 634 (1993).

<sup>14</sup>T.E. Mason *et al.*, Phys. Rev. Lett. **69**, 490 (1992).

<sup>15</sup>V. Jaccarino *et al.*, Phys. Rev. **160**, 476 (1967).

<sup>16</sup>Y. Ishikawa *et al.*, Phys. Rev. B **31**, 5884 (1985).

<sup>17</sup>D. Shinoda and S. Asanabe, J. Phys. Soc. Jpn. **21**, 555 (1966).

<sup>18</sup>Y. Takahashi and T. Moriya, J. Phys. Soc. Jpn. **46**, 1451 (1979).

<sup>19</sup>G. Shirane *et al.*, Phys. Rev. Lett. **59**, 351 (1987).

<sup>20</sup>D. Mandrus *et al.*, Phys. Rev. B **51**, 4763 (1995).

<sup>21</sup>B.C. Sales *et al.*, Phys. Rev. B **50**, 8207 (1994).

<sup>22</sup>C.H. Park *et al.*, Phys. Rev. B **52**, R16 981 (1995).

<sup>23</sup>C. Fu, M.P.C.M. Krijn, and S. Doniach, Phys. Rev. B **49**, 2219 (1994).

<sup>24</sup>A. Chainani *et al.*, Phys. Rev. B **50**, 8915 (1994).

<sup>25</sup>G.R. Castro *et al.*, J. Phys.: Condens. Matter **9**, 1871 (1997).

<sup>26</sup>W. Speier *et al.*, Phys. Rev. B **39**, 6008 (1989).

<sup>27</sup>S.J. Oh, J. Allen, and J.M. Lawrence, Phys. Rev. B **35**, 2267 (1987).

<sup>28</sup>A. Kakizaki *et al.*, J. Phys. Soc. Jpn. **51**, 2597 (1982).

<sup>29</sup>J.J. Hinarejos *et al.*, Phys. Rev. B **55**, 16 065 (1997).

<sup>30</sup>E. Weschke *et al.*, Phys. Rev. Lett. **69**, 1792 (1992).